Climate change implications for olive flowering in Crete, Greece: projections based on historical data

Manolis G. Grillakis[1] · Evangelos G. Kapetanakis[2] · Eleni Goumenaki[2]

Abstract

Climate change is expected to pose major challenges for olive cultivation in many Mediterranean countries. Predicting the development phases of olive trees is important for agronomic management purposes to foresee future climate impact and proactively act toward adaptation and mitigation strategies. In this study, a statistical model was developed based on winter chill accumulation and, in sequence, on heat accumulation to assess the changes in flowering occurrence for *Olea europaea* cv. Koroneiki, in the island of Crete, Greece. The model was based on and calibrated with long-term phenological observations and temperature data from four different sites in the island, spanning an elevation gradient between 45 and 624 m a.s.l. This model was used to assess the changes in flowering emergence under two Representative Concentration Pathway scenarios, RCP4.5 and RCP8.5, as projected by seven high-resolution Euro-CORDEX Regional Climate Models. Changes in chill accumulation were determined using the Dynamic Model. Reduction rates in chill accumulation for the whole chilling season ranged between 12.0 and 28.3% for the near future (2021–2060) and 22.7 and 70.9% for the far future (2061–2100), in comparison to the reference period of 1979–2019. Flowering was estimated to occur between 6 and 10 days earlier in the near future and between 12 and 26 days earlier in the far future, depending on the elevation and the climate change scenario.

✉ Evangelos G. Kapetanakis
   ekapet@hmu.gr

✉ Eleni Goumenaki
   egoumen@hmu.gr

[1] Laboratory of Geophysical-Remote Sensing and Archaeoenvironment, Institute for Mediterranean Studies, Foundation for Research and Technology Hellas, 74100 Rethymnon Crete, Greece

[2] School of Agricultural Sciences, Hellenic Mediterranean University, P.O. Box 1939, 71004 Heraklion, Crete, Greece

🖄 Springer

1 Introduction

Olive oil and edible olives are among the most important agricultural products in the Mediterranean region (Arcas et al. 2013). *Olea europaea* (Linnaeus), the olive tree, is one of the most cultivated tree species in the region, with a very high economic, social, and ecological importance (Rhizopoulou 2007). Crete is the fifth largest island of the Mediterranean Sea with a considerable olive oil production. Olive has been cultivated in Crete since Minoan times (from ca. 3500 BC; Boardman 1976). Its oil constituted a dominant agricultural product for the centuries that followed in historical times, as it does today for Crete and Greece. Koroneiki olive cultivar is of Greek origin, accounting for more than 55% of olive groves in the country (International Olive Council, 2021). It is the most prized cultivar for its Extra Virgin oil, of Protected Denomination of Origin for the most part of its production, in the island and for the whole country (Kosma et al. 2016). Koroneiki is also grown in many other countries around the Mediterranean Sea (Albania, Algeria, Cyprus, Egypt, France, Israel, Italy, Morocco, Portugal, Spain, Syria, Tunisia, Turkey) and in other countries with Mediterranean-type or temperate climates, e.g., Argentina, Australia, Brazil, Chile, China, Mexico, New Zealand, Peru, Saudi Arabia, South Africa, USA, and Uruguay (Bartolini 2008; International Olive Council 2021).

The Mediterranean Basin stretches between North Africa, with high temperatures and low rainfall, and the more rainy, temperate regions of Southern Europe and the Middle East. As a result, this area is often affected by interactions between sub-tropical and mid-latitude climate-change processes (D'Agostino et al. 2020). Climate change is expected to increase annual temperatures, especially in the southern parts of Europe, by the end of the twenty-first century (Arias et al. 2021). Projections regarding the southeastern Mediterranean region show an increase between 1.7 and 2.5 °C for the Representative Concentration Pathway of 4.5 W/m^2 (RCP4.5) scenario, and between 3.5 and 5 °C for the higher-end RCP 8.5 (Zittis et al. 2019).

A very important site feature for orchards is the sequence of seasonal temperatures in relation to the needs of tree crops. In temperate regions, fruit and nut tree species have chill requirements that need to be fulfilled to achieve regular crop yields (Luedeling et al. 2009). The annual olive fruiting process is a series of events that starts in the previous vegetative period and is affected by temperature sequensation. Olive flower induction commences in the summer (Fabbri and Benelli 2000). Later, under colder conditions, growth of the tree shoot meristems is stopped, sensitive tissues are protected in the buds, and the dormancy period starts (Dennis 1994). In relation to olive tree dormancy, three phases have been documented (Ramos et al. 2018; Rojo et al. 2020): (1) *paradormancy*, as the period of bud dormancy induced by the subtending leaves or a structure other than the buds; (2) *endodormancy* or *chilling*, when growth is suspended and trees accumulate chill so that their requirements are fulfilled; and (3) *ecodormancy* or *forcing* when, after sufficient exposure to higher temperatures, growth resumes. It is widely accepted that the most important signal for re-growth is temperature (Heide and Prestrud 2005). From the end of the winter, trees must be exposed to higher temperatures, resulting in the break of the dormant period, the activation of dormant tissues, shoot growth, and flowering (Fraga et al. 2020a). Olive cultivar genotype and its local adaptation define thermal requisites whereas latitude, longitude, and elevation are among the most important factors that modulate

the fulfillment of the thermal requisites of the olive tree (Aguilera et al. 2014; Rojo et al. 2020), although, so far, tree chill and heat needs generally have not been reliably quantified (Chuine et al. 2016; Lorite et al. 2020). A number of studies have linked changes in the chilling process with impacts on the quantity and quality of flowering that subsequently may affect olive production (Torres et al. 2017; Koubouris et al. 2019; Benlloch-González et al. 2019).

The bioclimatology of olive has been studied via various bioclimatic indices including the compensated thermicity index, the simple continentality index, and the annual ombrothermic index (Piñar Fuentes et al., 2019; Rivas-Martínez et al. 2002). These have been used mainly to study the bioclimate but not to quantify the effect of the climatic indices on the physiological parameters. Galán et al. (2005) used the accumulated growing degree-days (GDD), required after the chilling period, to initiate flowering. They calibrated the threshold temperature that signals the end of the chilling period and the start of the GDD accumulation for five sites in Spain. Their results indicate that the threshold temperature varies between higher and lower ground regions. Lower threshold temperatures were found at higher elevations. Aguilera et al. (2014) have also found that there is an adaptive biological response related to the biothermic requirements that differentiates olive crops over Mediterranean regions.

Chill accumulation is measured using different approaches. Three different models have been mainly used in calculating olive requirements, i.e., the Chilling Hours model (Bennett 1949; Weinberger 1950), the Utah model (Richardson et al. 1974), and the Dynamic Model (Fishman et al. 1987a, b; Luedeling et al. 2013). Comparisons of the different models for olive have not given consistent results (Rojo et al. 2020). Luedeling and Brown (2011) concluded that the Chilling Hours and Utah models need amendments related to location for successful use in estimating the impact of climate change on tree crops. Campoy et al. (2012) compared different chill accumulation approaches for apricot in the Mediterranean area and found that the Dynamic Model was more accurate in estimating the chill requirements. Another recent study on vineyards and olives concluded that the Dynamic Model for computing the Chill Portions (CP) is an advanced chilling model and that the Growing Degree Hours (GDH) model has been proven as more accurate than other models employing GDD (Fraga et al. 2019).

Olive orchards in the Mediterranean are at risk as, under higher future temperatures, they may not fulfill their chill requirements (Fraga et al. 2020b). Higher temperatures may lead to earlier and shorter phenological stages that could affect yields and quality characteristics (Bonofiglio et al. 2009; Garcia-Mozo et al. 2009). Olive groves have a long productive lifespan and high investments are involved. To sustain olive production in the current high yield areas, adaptation and mitigation strategies for the climate change may prove necessary. To this end, it is essential to estimate and quantify potential temperature changes in relation to olive cold and heat requirements for the near and far future.

Objectives of this research were (a) to develop, calibrate, and validate a statistical model to determine the dates of olive tree flowering in Crete by utilizing data from many consecutive years of phenological observations and temperature records, employing well-established techniques and (b) to make use of the model to assess changes in flowering timing under two global warming scenarios, utilizing an ensemble of seven high-resolution Regional Climate Models.

2 Methods and data

2.1 Study region

The study was carried out in the island of Crete, Greece (Fig. 1). The island covers 8336 km², accounting for 6.3% of the total Greek land area, with a population of 633,000 inhabitants (2018 census). It is located at the southern edge of the Aegean Sea, at about 160 km from the mainland. The island exhibits Mediterranean climate with long and dry summers and wet and mildly cold winters. Crete has steep topography with elevation varying up to 2456 m a.s.l. The olive groves of Crete account for 26.7% of the total olive area cultivation in Greece (213,521 ha) according to Corine Land Cover maps of 2018 (Kosztra et al. 2019).

2.2 Phenological observations

Phenological observations on the Koroneiki olive cultivar were recorded from 1984 to 2018 by the Regional Plant Protection and Quality Control Centre of Heraklion, Crete, a regional center affiliated to the Hellenic Ministry of Rural Development and Food. A total of ca. 1200 olive phenology observations, between the latent bud and the endocarp lignification stages, were recorded in olive groves at Gazi, Dafnes, Kastelli, and Aghia Varvara at elevations 45, 315, 340, and 624 m a.s.l. (Fig. 1). Phenology records for the four sites numbered 498 (from 1987 to 2018), 307 (from 1999 to 2018), 178 (from 1984 to 1998), and 164 (from 2007 to 2018), respectively. Table S1 in Online Resource (i.e., supplementary information including detailed data in tables and graphs) includes coordinates for the four sites. The times of emergence of each phenological stage for all sites are shown in Online Resource Fig. S5. In bioclimatic terms, all observation sites lie within the Mediterranean macroclimate, according to the classification proposed by Rivas-Martínez et al. (2017). Phenology was recorded using the phenological scale of Colbrant and Fabre (1981). On this scale, phenophases are symbolized with lettering from A to J, from latent buds to fully grown fruit, respectively. To facilitate statistical analysis, numbers were assigned to the Colbrant and Fabre letter symbols (Online Resource Table S2, Fig. S1). The conversion was tested for linearity using the GDH accumulation from the peak of the Chill Portions accumulation (Online Resource Fig. S6).
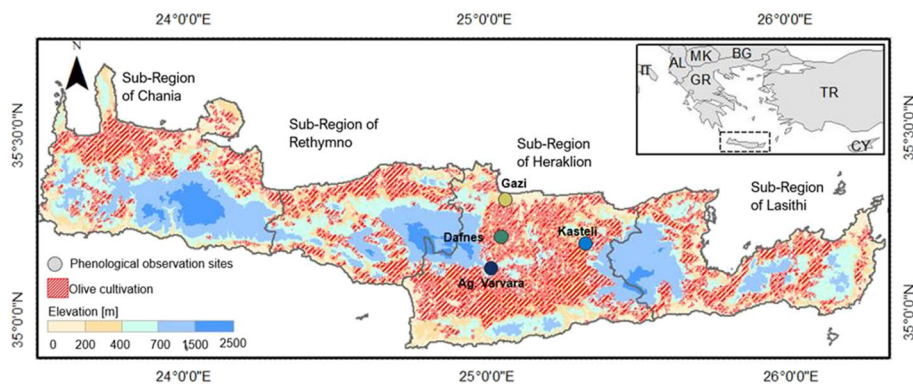
Fig. 1 The island of Crete. Different colors denote elevation gradient. Hatched areas show olive cultivation as on the Corine Land Cover map of 2018. Observation sites (see Sect. 2.2 below) are marked by dots

2.3 Chill and heat accumulation

The chill accumulation was assessed using the Dynamic Model (Fishman et al. 1987a, b). This model computes chill as Chill Portions in a two-step procedure. Cold temperatures promote the formation of a precursor which can be converted into a permanent Chill Portion if moderate temperatures prevail. This process is potentially reversible. The precursor can be removed if higher temperatures follow its formation, but once the precursor has reached a certain threshold, warmer temperatures do not hinder its irreversible transformation into a Chill Portion. The Chill Portions are potentially accumulated through late autumn and winter. In this study, the implementation of the Dynamic Model followed the MATLAB codes provided in Rodríguez et al. (2019). The peak chill date was found by estimating the centered 30-day moving average of the Chill Portions, between September and May.

The heat accumulation was computed as GDH, based on the approach of Gu (2016). They use sub-daily temperature data. In order to estimate GDH, records of minimum and maximum daily temperatures were used to disaggregate daily temperature values to hourly values, following the methodology of Wit (1978). The base temperature above which the GDH are accumulated was calibrated, as described in Sect. 2.4. In this study, the implementation of the GDH followed the MATLAB implementation of Ault et al. (2015).

2.4 Regression model for the flowering date determination

The statistical model developed in this study follows the concept that floral bud dormancy release occurs after olive trees have been exposed to a long enough period of chilling temperatures (Rallo and Martin 1991). It is based on the assumption that chill accumulates to break endodormancy and then heat accumulates to overcome quiescence phases, i.e., ecodormancy (De Melo-Abreu et al. 2004). First, the winter chill was calculated using the Dynamic Model and the day of the peak chilling was assessed. Then heat accumulation was determined, as GDH, until the onset of each observed phenological stage. For this procedure, two variables were calibrated, the base temperature above which the GDH are accumulated and the day from which onwards warmer temperature accumulation is calculated in relation to the peak of chilling. This approach was also followed by Aguilera et al. (2014), who calibrated the start date for the onset of the heat accumulation period in relation to the date of peak chilling. This procedure does not exclude chill accumulation beyond the day GDH start accumulating.

The optimization of the above two variables (base temperature for GDH accumulation and days to start counting GDH) was achieved by testing base temperatures between 1 and 25 °C in 0.5-°C steps. This is a wider range compared to test ranges found in the literature, e.g., 5 to 12.5 °C used by Galán et al. (2005), 4 to 15 °C used by Orlandi et al. (2006), and fixed 4.7 °C used by Pérez-López et al. (2008). GDH accumulation was tested with starting dates between − 50 and + 50 days from the date of peak chilling.

Heat accumulated up to each phenological observation was then correlated to the phenological phase using linear regression. The best-performing regression model was obtained by estimating the root mean square difference (RMSD) between the observed day of the year (DoY) that each phenological observation was recorded and the DoY simulated by the linear model. The RMSD is shown in Eq. (1).

$$RMSD = \sqrt{\frac{\sum_1^n (DoY_{pheno}^{OBS} - DoY_{pheno}^{SIM})^2}{n}} \qquad (1)$$

DoY_{pheno}^{OBS} is the day of the year when each of the n phenological stages was observed across the observation years for each site. DoY_{pheno}^{SIM} is the day of the year when the respective phenological stage was determined by the regression procedure. The calibration was based on the minimization of the RMSD. This optimization approach has been widely used, e.g., by Rojo et al. (2020) and Aguilera et al. (2014). The calibration procedure results in an average number of GDH that must be accumulated to reach each phenological stage.

The phenological records were randomly split into two different sets of whole-year data, to calibrate and validate the regression models. For the calibration, 70% of the data were used, allowing 30% for validation. The procedure was performed for each of the four sites separately and was repeated 10 times to secure that the data selection did not bias the calibration–validation procedure. Tables S3 to S6 in Online Resource show the random years used for calibration and validation for each study site. This methodology follows the calibration–validation procedure of Grillakis et al. (2020).

For the climate projection data, to estimate the flowering date, winter chill, as Chill Portions, and the date of peak chilling were determined. Then the GDH were summed, starting from the calibrated date relative to the peak of chilling, until the calibrated number of GDH for the emergence of the F phenological stage was reached. This procedure was repeated for all study sites.

2.5 Temperature data

2.5.1 Recorded temperatures

Temperatures were recorded at the four sites (Online Resource Table S1) by the Regional Center for Plant Protection, Quality and Phytosanitary Control of Heraklion, Crete. A few missing temperature values at the four phenology observation sites were filled in using datasets from another 63 weather stations distributed on the whole island of Crete, operated and calibrated by the Hellenic National Meteorological Service and the National Observatory of Athens. The missing values were filled in by interpolating the data of the above three weather station networks into a regular 100-m resolution dataset following the procedure described in detail by Grillakis et al. (2022).

2.5.2 Projected regional climate models

Simulated daily temperature data of seven high-resolution Regional Climate Models (RCMs), participating in the Coordinated Regional Downscaling Experiment for Europe initiative—Euro-CORDEX 0.11° or EUR-11 (Jacob et al. 2013), were used as listed in Online Resource Table S7. Two Representative Concentration Pathways (RCPs) (Moss et al. 2010; O'Neill et al. 2014) for the future were considered, the mid-range climate change RCP4.5 (Wise et al. 2009) and the high-end climate change scenario RCP8.5 (Riahi et al. 2011). The above RCMs have been widely used for climate change impact assessment in the Mediterranean region for their fine spatial resolution and the existence of many model simulations (e.g., Mascaro et al., 2018; Grillakis et al. 2020; Molina et al. 2020).

The model employed in the present study followed Jacob et al. (2018) with few modifications and enrichment with more simulations. Two 40-year periods were considered, one for the near future (NF; 2021–2060) and one for the far future (FF; 2061–2100), and these were compared against the historical period of 1980–2019.

Daily RCM temperature data were adjusted for their biases using Multi-segment Statistical Bias Correction (MSBC) (Grillakis et al. 2013, 2017). This was considered necessary because raw climate model simulations often include biases in the mean and the annual distribution, compared to the observations (Christensen et al. 2008; Haerter et al. 2011). The methodology is a quantile mapping technique with trend preservation. Advantages and drawbacks of the quantile mapping family of methods have been widely discussed in the literature, e.g., Maraun et al. (2010) and Themeßl et al. (2011). The bias adjustment transfer function was calibrated between the RCM simulated and the observed data of the 1979–2019 period. Since EUR-11 historical simulation period ends at 2005, with 2006 onwards simulations being forced by the RCP forcing, the bias adjustment was performed twice for the baseline period, i.e., once for 1979–2005 complemented with the RCP4.5 between 2006 and 2019 and once more with RCP8.5 for the same period.

3 Results

3.1 Temperature trends, winter chill, and RCM projections

Annual temperature data showed a statistically significant increasing trend, ranging between 0.36 and 0.40 °C per decade across all sites, with a 95% confidence interval between 0.23 and 0.53 (Online Resource Fig. S3a). Mean annual temperatures of the period from October to May, which mainly affect the flowering process of olive trees, followed a similar trend (Online Resource Fig. S3b). Accumulated Chill Portions per season ranged between 50.6 CP (for Gazi) and 97.3 CP (for Aghia Varvara), with a decreasing trend between 0.53 and 0.70 CPs per year (Online Resource Fig. S3c). The distribution of the daily maximum and minimum temperatures per site and per month is shown in Online Resource Fig. S2. The accumulated Chill Portions showed a correlation with the flowering process. Increased Chill Portions accumulation, either until the day of peak chilling accumulation or until the end of winter, was shown to be positively correlated to a delay in the flowering process among the four sites, following the increasing elevation gradient (Online Resource Fig. S4).

The temperature data used in the model of this study were adjusted for bias toward the reference period observed temperatures. Figure 2a shows the mean annual temperature, averaged across the four sites, prior and after the application of the bias correction. The raw RCM temperature underestimates the mean annual temperature by 1.5 °C (from 17.1 to 15.6 °C) in the reference period 1979–2019. On average, climate change is expected to increase the temperature in the area of the case study sites by 0.96 and 1.3 °C under RCP4.5 and RCP8.5, respectively, for the near future and by 1.6 and 3.3 °C under the RCP4.5 and RCP8.5 for the far future. Figure 2b and c show the changes in the adjusted seasonal temperature in the near and far future, respectively. In Fig. 2d and e, the seasonal differences are shown in comparison to the reference period. The expected changes in the mean temperatures in the near future period range between 1.0 and 1.5 °C. In the far future period, the RCP4.5 change ranges between 1.5 and 2.0 °C. For the RCP8.5, the temperature
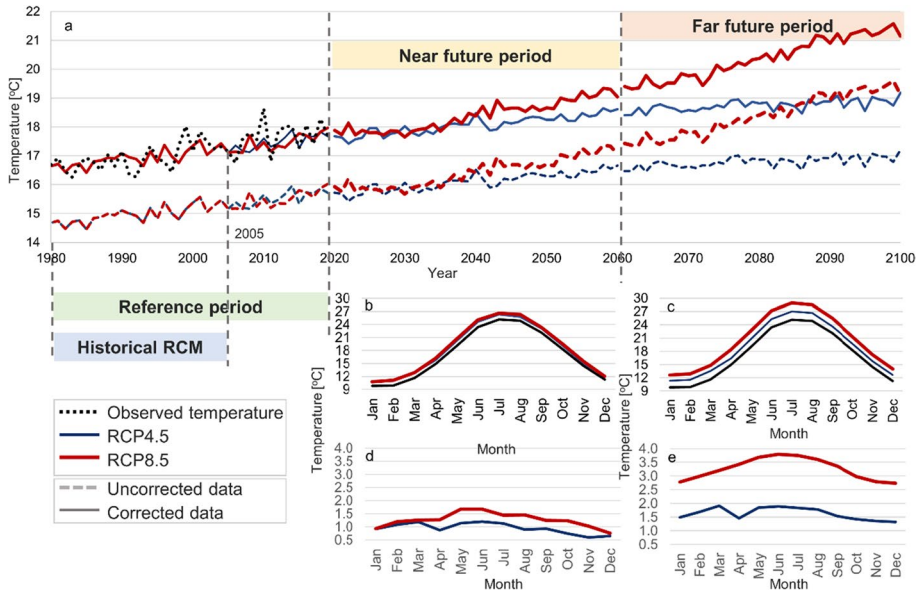
Fig. 2 Mean annual temperatures (**a**) for the observation period (dotted line), for RCP4.5 (thin lines), and for RCP 8.5 (thick lines), for the raw data (dashed lines) and the bias-adjusted data (solid lines). Graphs (**b**) and (**c**) depict the comparison between the monthly seasonal mean temperatures of the observed (dotted line), bias-corrected RCP4.5 (solid thin line) and RCP8.5 (solid thick line) temperatures, for the near future (**b**) and far future (**c**) periods. Graphs (**d**) and (**e**) show the respective changes of (**b**) and (**c**) in comparison to the observed data for the near future and the far future periods, for the bias-corrected RCP4.5 (solid thin line) and RCP8.5 (solid thick line) temperatures. All the *y*-axis units are in degrees Celsius

projection increase reaches ca. 4 °C for the summer months. The climate change signal was analyzed for the mean daily temperature and the bias adjustment procedure was repeated for the minimum and maximum daily temperature data, as required for the application of the dynamic chilling model and the determination of heat accumulation. It is worth noting that the interannual variability of the RCM ensemble members is canceled out in the ensemble mean (Fig. 2a); hence, the variability of the observations in Fig. 2a is shown to be much higher compared to the ensemble averages.

3.2 Regression model calibration and validation

The calibration procedure provided the optimal base temperature, in terms of RMSD, and the day to start counting GDH in relation to the day of peak Chill Portions accumulation. The optimal base temperature values obtained were 10, 11.5, 11, and 7.5 °C for Gazi, Dafnes, Kasteli, and Aghia Varvara, respectively. The optimal day to start calculating heat accumulation was the 10th, 5th, − 5th, and 15th day of the year for the above locations. The RMSD ranged between 8.89 and 13.31 days for the calibration and 9.39 and 13.75 days for the validation, among all the phenological stages. The split sample calibration and validation results for the optimal model parameters are detailed in Online Resource Tables S3 to S6. Regarding the onset of flowering (phenological phase F), the RMSD was estimated at 9.64, 4.12, 6.45, and 3.67 days for Gazi, Dafnes, Kasteli, and Aghia Varvara sites, respectively (see Online Resource Table S8 for the rest of the phenological phases). Figure 3

shows the RMSDs obtained for each base temperature tested, and each day to start calculating heat accumulation, using all the available data for each location.

The scatter plots in Fig. 4a–d show the GDH accumulates in relation to the peak of chilling against the phenological phases. Graphs e, f, g, and h show phenological phases simulated by the linear model developed in this study against the observed phenophases. The simulated DoY of emergence of the phenological stages against the observed DoY are shown in Fig. 4i–l. In this study, the optimization was based on the least RMSD regarding the observed versus simulated DoY for each phenological phase (Fig. 4i–l). The R^2 of the regression between each phenological phase and the corresponding accumulated observed GDH is depicted in Fig. 4a–d. The correlations showed a good fit, with R^2 ranging between 0.82 and 0.91 for the four sites.

Normal probability plots of residuals were constructed for the optimized linear models of Fig. 4a–d to examine the validity of the linear relationships developed
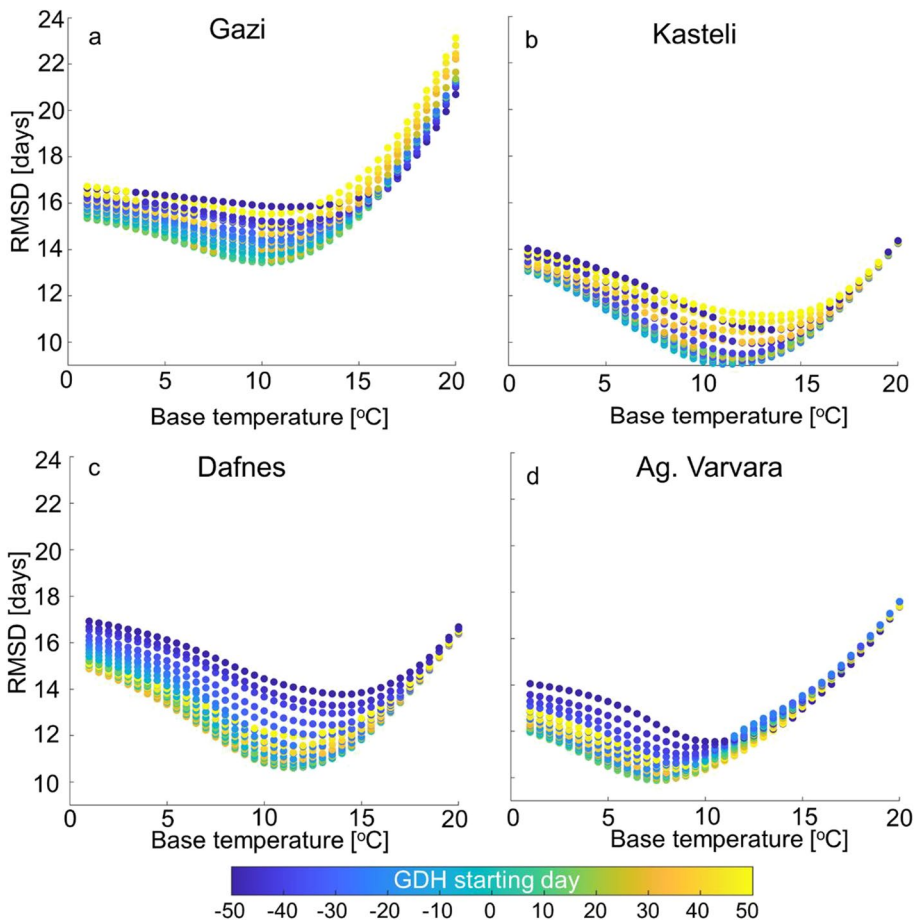
Fig. 3 Day to start calculating heat accumulation after the day of peak chilling accumulation. The RMSD (*y*-axis) between the observed and simulated emergence day of each phenological stage is plotted against the different base temperatures (*x*-axis) and the day to start calculating heat accumulation for each of the four locations examined. Day 0 represents the day of peak Chill Portion accumulation. RMSD values presented in the *y*-axis were obtained using the whole validation and calibration data set
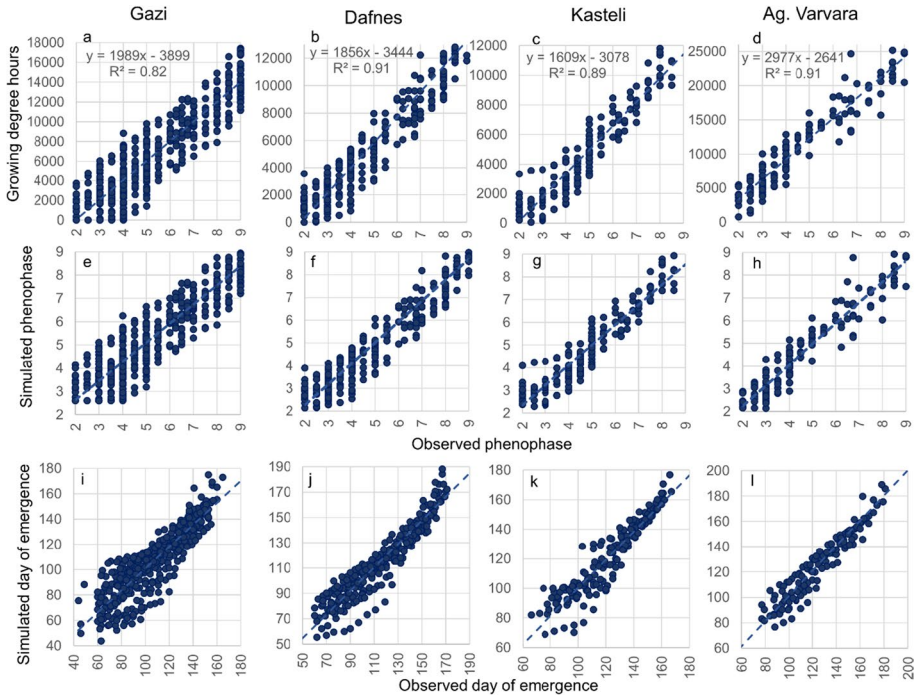
Fig. 4 Scatter plots of phenological phases, day of emergence, and GDH. Upper row graphs show heat accumulation (in GDH units) in relation to the peak of chilling vs. the observed phenophases. Middle row graphs show the simulated vs. the observed phenophase as estimated by the linear regressions of the data depicted in the graphs of the upper row. Lower row graphs show simulated day of emergence of each phenophase (day of the year starting from 1st of January), a product of the linear regressions of the data depicted in the graphs of the upper row, vs. observed day of emergence

(Online Resource Fig. S6). The residuals are normally distributed, showing that the linear regression between accumulated GDH and the phenophase is valid. This correlation approach exhibits a weakness when each phenophase is transformed from the categorical scale of Colbrant and Fabre into a numerical one (Fig. 4e–h, x-axis), i.e., while for each phenophase a range of Growing Degree values were estimated depending on the different years of observation, the regression model does not simulate this variability, assigning a single heat accumulation value for each phenological stage. The calculated GDH accumulated for phenophase F—"first flowers open"—were 8835, 8336, 7220, and 16,415 GDHs for Gazi, Dafnes, Kasteli, and Aghia Varvara, respectively, in relation to the site-specific base temperatures.

3.3 Climate-driven changes in chill accumulation

The RCM-based temperature projections showed a significant loss in the chill accumulation, both up to the day of maximum Chill Portion accumulation and for the whole cold season (Fig. 5). Median chill accumulation reduction until maximum accumulation date, across the above scenarios, varies between 8.8 and 28.6% for the near future and between
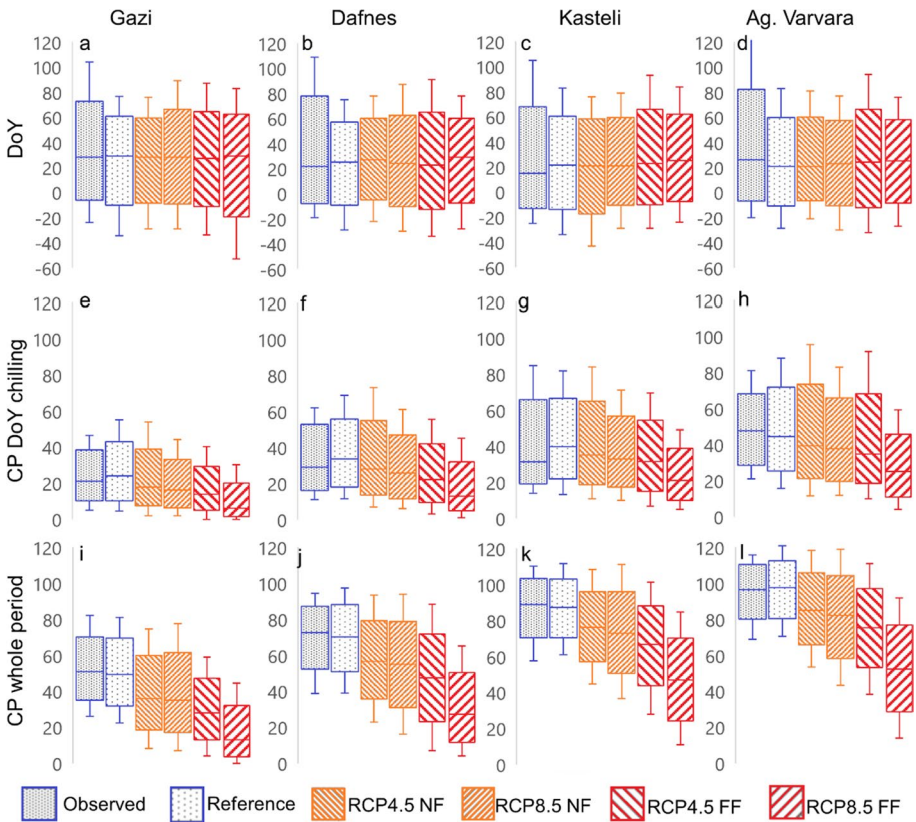
Fig. 5 Day of the year of peak chill accumulation (in CP units) and chill accumulation to the day of peak chilling or for the whole period. Chill accumulation is shown, for the observations and the reference period in the model, for near future (NF) and far future (FF), and RCP4.5 and RCP8.5 scenarios. Graphs (**a**) to (**d**) show Chill Portions to the day of the year on which the peak chill accumulation is estimated. Graphs (**e**) to (**h**) show the Day of the Year (DoY—starting from January 1st) when the peak Chill Portion accumulation occurs. Graphs (**i**) to (**l**) show Chill Portions accumulated for the whole period**.** The boxplots of the model data (reference period, NF and FF) are estimated on all seven RCM data, binned

20.2 and 72.0% for the far future, across all four sites. The respective reduction rates for the whole chilling season vary between 12.0 and 28.3% for the near future and 22.7 and 70.9% for the far future. The impact on chill accumulation is projected to be more severe in the study sites that exhibit higher temperatures, i.e., Gazi and Dafnes. It is worth noting that. under the RCP8.5 projection for the far future, the results showed that in areas located at the lowest elevation, i.e., Gazi, Chill Portions are expected to practically nullify for some years (Fig. 5e, i). The day of the year of peak Chill Portion accumulation did not vary considerably in comparison to the reference period. The median difference ranged between -2 and 4 days across different periods, sites, and scenarios (see Online Resource Table S9).

Chill Portions determined through the bias adjusted RCM data are very similar to those observed in the reference period, both for the Chill Portions accumulated up to the day of maximum chilling accumulation and for the entire period (Fig. 5).

3.4 Climate-driven changes in flowering emergence

The flowering day of the year, i.e., phenophase F on the Colbrant and Fabre scale, was estimated for the reference period by applying the established regression relationships on the RCM data. The observed average day of flowering is generally close to the day estimated through the RCM data, with deviations of 4, 11, −4, and 7 days for Gazi, Dafnes, Kasteli, and Aghia Varvara, respectively (Table 1). The flowering day for each year for the individual RCM models and the median day among the models for RCP4.5 and RCP8.5 are detailed in Online Resource Fig. S7. In near future, flowering emergence is expected to occur earlier by 6 to 10 days on average, depending on the scenario and the site of records (Table 1). Changes in the far future are expected to be more significant, with flowering emergence occurring 12 to 26 days earlier. The observed flowering days, detailed in Online Resource Fig. S7, were found to be within the range of the different RCMs. Results did not show a clear trend in all cases. The signal seems to be stronger for Gazi due to the long period of records.

4 Discussion

A statistical model was calibrated and validated to assess climate change impact on olive tree flowering for the very broadly cultivated cv. Koroneiki in the island of Crete, Greece. The model was based on observations of 12 to 31 years from four different sites in the island, at an elevation gradient from 45 to 624 m a.s.l. The model was used to estimate possible differentiations related to fulfillment of olive tree thermal requirements due to climate change, focusing on the prediction of the onset of flowering under different climate pathways. This model was based on the sequence of chill and heat accumulation, using the Dynamic Model and the Growing Degree Hours approaches, respectively. Two parameters were calibrated in relation to the day of maximum Chill Portion accumulation, the base temperature above which heat is accumulated and the starting day of heat accumulation. The resulting base temperatures varied across the study sites between 7.5 and 11.5 °C, with the lowest threshold temperature corresponding to the highest elevation (Aghia Varvara), similarly to the findings of Galán et al. (2005). The optimal DoY to start counting GDH varied between 27 December and 15 January. Linear regression was performed between

Table 1 Median flowering day of the year, i.e., DoY in which phenophase F of Colbrant and Fabre scale emerges, for the observation and reference periods, near and far future, RCP4.5 and RCP8.5, for each of the four observation sites

	Gazi		Dafnes		Kasteli		Aghia Varvara	
Observed	118		129		140		145	
Reference	122		140		136		152	
	RCP4.5	RCP8.5	RCP4.5	RCP8.5	RCP4.5	RCP8.5	RCP4.5	RCP8.5
Near future	114 (−8)	113 (−9)	133 (−7)	130 (−10)	1129 (−7)	1260 (−10)	146 (−6)	143 (−10)
Far future	108 (−14)	99 (−23)	126 (−13)	115 (−25)	123 (−13)	110 (−26)	140 (−12)	129 (−23)

the accumulated GDH and the observed day of flowering emergence. The two parameters were optimized with the aim to minimize the error in the flowering day determination. The optimal linear models, one for each of the four case study sites, obtained RMSD values between 8.89 and 13.31 days. The normal probability plots of residuals showed that linear regression well approximates the correlation. This finding has a twofold importance, the conversion of the phenological phases from categorical to numerical scale employed in the model is valid, and the use of the GDH well approximates the determination of flower emergence. This latter result is in agreement with the findings of Elloumi et al. (2020) and Rojo et al. (2020).

A strong decrease in the winter chill accumulation was found, with RCP8.5 being the worst-case scenario in both near and especially in the far future periods. Our findings indicate that chill accumulation at the upper elevation margin of olive cultivation in Crete, as in Aghia Varvara, will potentially exhibit a drastic reduction of ca. 45% and will be lowered to current chill counts at sea level, as in Gazi. Furthermore, a significant outcome of the chill accumulation estimates is that the lower quartiles of chill are close to zero, especially for RCP8.5 and the far future period. This extremely low chill accumulation may not prove adequate for the induction of flowering in Koroneiki or other olive cultivars of similar temperature adaptations. Koroneiki olive cultivar has also been the subject of other research studies in relation to its suitability in projected climate scenarios (Gabaldón-Leal et al. 2017; Koubouris et al. 2019). In comparison, the present study appears to have a higher value as our analyses are based on field observations up to 31 years, whereas the above two studies consist of experimentation on potted plants, including outdoor and greenhouse treatments for a limited time.

Another interesting finding of this study, in all four sites, was that the day of the peak Chill Portion accumulation does not appear to shift significantly. As a consequence, the earlier emergence of olive flowering is mainly governed by higher temperatures that result in a faster Growing Degree Hour gain rate. Flowering emergence was found to be advanced by 6 to 10 days on average in the four different locations in the near future and by 12 to 26 days in the far future. Advancement of flowering emergence, as a result of projections in this and other studies (Orlandi et al. 2010; Rojo et al. 2020), may expose sensitive growth stages to risks of damage due to extreme weather events occurring at higher frequencies, e.g., surges of higher temperatures, frosts, and extreme precipitation events.

Our results show that climate warming will have a significant impact on olive and potentially on other tree crops in the Mediterranean region and in other areas with Mediterranean type climates. These results are in line with those of previous studies (Giorgi and Lionello 2008; Guiot and Cramer 2016; Santos et al. 2017). Rising temperatures may lead to gaps in fulfilling chill requirements in late autumn and early winter. Failure to meet temperature requirements will potentially result in changes in the quality and quantity of olive production. These conclusions are in agreement with those of several other researchers (Moriondo et al. 2015; Koubouris et al. 2019; Fraga et al. 2019; Benlloch-González et al. 2019).

Projections by other researchers have also shown very significant reductions in chilling in other countries with Mediterranean type climates, e.g., Australia, South Africa, and the USA (Luedeling 2012). The assumed chilling requirements of the plants, together with these losses in chilling, constitute a grim outlook for many production areas, especially for those with higher temperatures. In many cases, crop adaptation does not appear possible. Selection of suitable plant cultivars for areas with projected dramatic temperature changes is likely to be very restricted because there are no reliable assessments of the chilling requirements of the different plant varieties. Luedeling and Brown (2011) reported that chilling

requirement estimates have been made for many plant cultivars in specified areas, but these estimates cannot be applied to areas other than those where they were determined. The value of these estimates is restricted by the fact that in the research literature there are serious gaps in our knowledge of the genetic mechanisms and the physiological processes that underlie tree dormancy and how any of these mechanisms may be modified and adapted. Crop adaptation could be approached through climate analogue analysis, i.e., (a) the search for climates among present-day areas that may have the main features of the projected climates and (b) simulation of adaptation activities from such areas, as an approach for securing that tree orchards maintain their productivity and financial sustainability in the projected periods of drastic climate changes in temperate regions (Luedeling 2012).

Research findings of Zouari et al. (2015) and Elloumi et al. (2020) in Tunis offer themselves for a climate analogue analysis. Temperatures in Tunis appear to be on average 2.5 °C higher than current temperatures at olive growing areas in Crete. This difference falls within the temperature differences of the climate change scenarios applied for Crete (Fig. 2). In Tunis, Elloumi et al. (2020) found that flowering occurred between 93 and 125 DoY. Throughout our observation period, flowering in Crete occurred on average between 121 DoY (Gazi) and 149 DoY (Aghia Varvara). This comparison leads to the conclusion that our estimated future temperature increase of 2.5 °C will potentially result in flower emergence occurring in Crete on Days of the Year similar to those that occur in Tunis today. Considering our specific findings about earlier flower emergence, the above comparison adds validity to the overall outcomes and conclusions of the present work.

A limitation of this study is that the effects of the projected climatic changes on olive flowering are analyzed only as a function of temperature, as the main driving factor. Other factors may also prove important, probably to a lesser extent, including water relations, wind regimes, and farm management practices. These factors and others of minor importance in relation to the purposes of this study could not be taken into consideration within the limits of the present research.

The model developed in the present study obtained satisfactory results in predicting the flowering day of the year for the olive tree cv. Koroneiki in Crete for a gradient of olive grove altitudes. The climatic changes, especially in relation to lower temperatures that contribute to chilling, could have a negative effect on the fulfillment of olive tree requirements for the break of endodormancy and eventually on flowering and fruit production in areas of low altitude in Crete and in other areas of Greece and other countries with Mediterranean-type climates. Therefore, a question arises as regards future suitability of current olive varieties in the high productivity areas they are grown at present or for future olive grove expansion. Adaptation and mitigation strategies are needed as well as further research on olive dormancy physiology, genetic material, and agronomic practices to proactively ameliorate the negative effect of increasing temperatures.

5 Conclusions

The application of the statistical model developed in this study suggested a noteworthy reduction in the chill accumulation across all climate projections and altitudes of the study sites and an earlier occurrence of the flowering phase. Predicted temperature increases in some areas may not allow the fulfillment of chilling requirements of the olive tree every year, for flowering and fruit production, and thus threaten the economic viability of olive cultivation in some regions of the Mediterranean. The combination of models based on

long-range temperature and phenology data with climate change projections constitutes a valuable tool for restructuring sustainable olive production systems. In this context, the present study lends support to ongoing efforts for climate change adaptation strategies for olive cultivation.

References

Aguilera F, Ruiz L, Fornaciari M et al (2014) Heat accumulation period in the Mediterranean region: phenological response of the olive in different climate areas (Spain, Italy and Tunisia). Int J Biometeorol 58:867–876. https://doi.org/10.1007/s00484-013-0666-7

Arcas N, Arroyo López FN, Caballero J, et al (2013) Present and future of the Mediterranean Olive Sector. In: IAMZ-CIHEAM, Options Méditerranéennes Series A: Mediterranean Seminars. pp 1–197

Arias PA (2021) Technical summary. In: Climate Change 2021: the physical science basis. Contrib. Work. Gr. I to Sixth Assess. Rep. Intergov. Panel Clim. Chang

Ault TR, Zurita-Milla R, Schwartz MD (2015) A Matlab© toolbox for calculating spring indices from daily meteorological data. Comput Geosci 83:46–53. https://doi.org/10.1016/j.cageo.2015.06.015

Bartolini G (2008) Olive germplasm (*Olea europaea* L.), cultivars, synonyms, cultivation area, collections, descriptors. https://doi.org/10.7349/OLEA_databases

Benlloch-González M, Sánchez-Lucas R, Bejaoui MA et al (2019) Global warming effects on yield and fruit maturation of olive trees growing under field conditions. Sci Hortic (amsterdam) 249:162–167. https://doi.org/10.1016/J.SCIENTA.2019.01.046

Bennett J (1949) Temperature and bud rest period: effect of temperature and exposure on the rest period of deciduous plant leaf buds investigated. Calif Agric 3:9–12

Boardman J (1976) The olive in the Mediterranean: its culture and use. Philos Trans R Soc London b, Biol Sci 275:187–196

Bonofiglio T, Orlandi F, Sgromo C et al (2009) Evidences of olive pollination date variations in relation to spring temperature trends. Aerobiologia 25:227–237. https://doi.org/10.1007/s10453-009-9128-4

Campoy JA, Ruiz D, Allderman L et al (2012) The fulfilment of chilling requirements and the adaptation of apricot (Prunus armeniaca L.) in warm winter climates: an approach in Murcia (Spain) and the Western Cape (South Africa). Eur J Agron 37:43–55. https://doi.org/10.1016/j.eja.2011.10.004

Christensen JH, Boberg F, Christensen OB, Lucas-Picher P (2008) On the need for bias correction of regional climate change projections of temperature and precipitation. Geophys Res Lett 35:L20709. https://doi.org/10.1029/2008GL035694

Chuine I, Bonhomme M, Legave JM et al (2016) Can phenological models predict tree phenology accurately in the future? The unrevealed hurdle of endodormancy break. Glob Chang Biol 22:3444–3460. https://doi.org/10.1111/GCB.13383

Colbrant P, Fabre P (1981) Stades repères de l'Olivier. In R. Maillard "L'Olivier." In: Comité Technique de l'Olivier. Section Spécialisée du C.T.I.F.L.

D'Agostino R, Scambiati AL, Jungclaus J, Lionello P (2020) Poleward shift of northern subtropics in winter: time of emergence of zonal versus regional signals. Geophys Res Lett 47:e2020GL089325

De Melo-Abreu JP, Barranco D, Cordeiro AM et al (2004) Modelling olive flowering date using chilling for dormancy release and thermal time. Agric for Meteorol 125:117–127. https://doi.org/10.1016/j.agrformet.2004.02.009

Dennis FG (1994) Dormancy—what we know (and don't know). HortScience 29:1249–1255

Elloumi O, Ghrab M, Chatti A et al (2020) Phenological performance of olive tree in a warm production area of central Tunisia. Sci Hortic-Amsterdam 259:108759. https://doi.org/10.1016/J.SCIENTA.2019.108759

Fabbri A, Benelli C (2000) Flower bud induction and differentiation in olive. J Hortic Sci Biotechnol 75:131–141

Fishman S, Erez A, Couvillon GA (1987a) The temperature dependence of dormancy breaking in plants: mathematical analysis of a two-step model involving a cooperative transition. J Theor Biol 124:473–483. https://doi.org/10.1016/S0022-5193(87)80221-7

Fishman S, Erez A, Couvillon GA (1987b) The temperature dependence of dormancy breaking in plants: computer simulation of processes studied under controlled temperatures. J Theor Biol 126:309–321. https://doi.org/10.1016/S0022-5193(87)80237-0

Fraga H, Pinto JG, Santos JA (2019) Climate change projections for chilling and heat forcing conditions in European vineyards and olive orchards: a multi-model assessment. Clim Change 152:179–193. https://doi.org/10.1007/s10584-018-2337-5

Fraga H, Moriondo M, Leolini L, Santos JA (2020a) Mediterranean olive orchards under climate change: a review of future impacts and adaptation strategies. Agronomy 11:56

Fraga H, Pinto JG, Santos JA (2020b) Olive tree irrigation as a climate change adaptation measure in Alentejo Portugal. Portugal Agric Water Manag 237:106193. https://doi.org/10.1016/j.agwat.2020.106193

Gabaldón-Leal C, Ruiz-Ramos M, de la Rosa R et al (2017) Impact of changes in mean and extreme temperatures caused by climate change on olive flowering in southern Spain. Int J Climatol 37:940–957. https://doi.org/10.1002/JOC.5048

Galán C, García-Mozo H, Vázquez L et al (2005) Heat requirement for the onset of the Olea europaea L. pollen season in several sites in Andalusia and the effect of the expected future climate change. Int J Biometeorol 49:184–188

Garcia-Mozo H, Orlandi F, Galan C et al (2009) Olive flowering phenology variation between different cultivars in Spain and Italy: modeling analysis. Theor Appl Climatol 95:385–395

Giorgi F, Lionello P (2008) Climate change projections for the Mediterranean region. Glob Planet Change 63:90–104. https://doi.org/10.1016/j.gloplacha.2007.09.005

Grillakis MG, Koutroulis AG, Tsanis IK (2013) Multisegment statistical bias correction of daily GCM precipitation output. J Geophys Res Atmos 118:3150–3162. https://doi.org/10.1002/jgrd.50323

Grillakis MG, Koutroulis AG, Daliakopoulos IN, Tsanis IK (2017) A method to preserve trends in quantile mapping bias correction of climate modeled temperature. Earth Syst Dynam 8:889–900. https://doi.org/10.5194/esd-8-889-2017

Grillakis MG, Polykretis C, Alexakis DD (2020) Past and projected climate change impacts on rainfall erosivity: advancing our knowledge for the eastern Mediterranean island of Crete. CATENA 193:104625. https://doi.org/10.1016/j.catena.2020.104625

Grillakis MG, Doupis G, Kapetanakis E, Goumenaki E (2022) Future shifts in the phenology of table grapes on Crete under a warming climate. Agric For Meteorol 318:108915. https://doi.org/10.1016/j.agrformet.2022.108915

Gu S (2016) Growing degree hours–a simple, accurate, and precise protocol to approximate growing heat summation for grapevines. Int J Biometeorol 60:1123–1134

Guiot J, Cramer W (2016) Climate change: the 2015 Paris Agreement thresholds and Mediterranean basin ecosystems. Science 354:465–468. https://doi.org/10.1126/SCIENCE.AAH5015

Haerter JO, Hagemann S, Moseley C, Piani C (2011) Climate model bias correction and the role of timescales. Hydrol Earth Syst Sci 15:1065–1079. https://doi.org/10.5194/hess-15-1065-2011

Heide OM, Prestrud AK (2005) Low temperature, but not photoperiod, controls growth cessation and dormancy induction and release in apple and pear. Tree Physiol 25:109–114. https://doi.org/10.1093/TREEPHYS/25.1.109

International Olive Council (2021) The International Olive Council – IOOC. https://www.internationaloliveoil.org/. Accessed 6 May 2021

Jacob D, Petersen J, Eggert B et al (2013) EURO-CORDEX: new high-resolution climate change projections for European impact research. Reg Environ Chang 14:563–578. https://doi.org/10.1007/s10113-013-0499-2

Jacob D, Kotova L, Teichmann C et al (2018) Climate impacts in Europe under +1.5°C global warming. Earth's Futur 6:264–285. https://doi.org/10.1002/2017EF000710

Kosma I, Badeka A, Vatavali K et al (2016) Differentiation of Greek extra virgin olive oils according to cultivar based on volatile compound analysis and fatty acid composition. Eur J Lipid Sci Technol 118:849–861

Kosztra B, Büttner G, Hazeu G, Arnold S (2019) Updated CLC illustrated nomenclature guidelines. European Environment Agency, Wien

Koubouris G, Limperaki I, Darioti M, Sergentani C (2019) Effects of various winter chilling regimes on flowering quality indicators of Greek olive cultivars. Biol Plant 63:504–510. https://doi.org/10.32615/bp.2019.065

Lorite IJ, Cabezas-Luque JM, Arquero O et al (2020) The role of phenology in the climate change impacts and adaptation strategies for tree crops: a case study on almond orchards in Southern Europe. Agric for Meteorol 294:108142. https://doi.org/10.1016/J.AGRFORMET.2020.108142

Loussert R, Brousse G (1978) L'olivier. Techniques agricoles et production méditerranéennes. Maisonneuve et Larose, Paris 460

Luedeling E (2012) Climate change impacts on winter chill for temperate fruit and nut production: a review. Sci Hortic-Amsterdam 144:218–229. https://doi.org/10.1016/J.SCIENTA.2012.07.011

Luedeling E, Brown PH (2011) A global analysis of the comparability of winter chill models for fruit and nut trees. Int J Biometeorol 55:411–421. https://doi.org/10.1007/s00484-010-0352-y

Luedeling E, Zhang M, Luedeling V, Girvetz EH (2009) Sensitivity of winter chill models for fruit and nut trees to climatic changes expected in California's Central Valley. Agric Ecosyst Environ 133:23–31

Luedeling E, Guo L, Dai J et al (2013) Differential responses of trees to temperature variation during the chilling and forcing phases. Agric for Meteorol 181:33–42. https://doi.org/10.1016/J.AGRFORMET.2013.06.018

Maraun D, Wetterhall F, Ireson AM, et al (2010) Precipitation downscaling under climate change: recent developments to bridge the gap between dynamical models and the end user. Rev Geophys 48:. https://doi.org/10.1029/2009RG000314

Mascaro G, Viola F, Deidda R (2018) Evaluation of precipitation from EURO-CORDEX regional climate simulations in a small-scale Mediterranean site. J Geophys Res Atmos 123:1604–1625. https://doi.org/10.1002/2017JD027463

Molina MO, Sánchez E, Gutiérrez C (2020) Future heat waves over the Mediterranean from an Euro-CORDEX regional climate model ensemble. Sci Rep 10:1–10. https://doi.org/10.1038/s41598-020-65663-0

Moriondo M, Ferrise R, Trombi G et al (2015) Modelling olive trees and grapevines in a changing climate. Environ Model Softw 72:387–401. https://doi.org/10.1016/J.ENVSOFT.2014.12.016

Moss RH, Edmonds JA, Hibbard KA et al (2010) The next generation of scenarios for climate change research and assessment. Nature 463:747–756. https://doi.org/10.1038/nature08823

O'Neill BC, Kriegler E, Riahi K et al (2014) A new scenario framework for climate change research: the concept of shared socioeconomic pathways. Clim Change 122:387–400. https://doi.org/10.1007/s10584-013-0905-2

Orlandi F, Lanari D, Romano B, Fornaciari M (2006) New model to predict the timing of olive (Olea europaea) flowering: a case study in central Italy. New Zeal J Crop Hortic Sci 34:93–99. https://doi.org/10.1080/01140671.2006.9514392

Orlandi F, Garcia-Mozo H, Vazquez Ezquerra L et al (2010) Phenological olive chilling requirements in Umbria (Italy) and Andalusia (Spain). Plant Biosyst - Int J Dealing Asp Plant Biol 138:111–116. https://doi.org/10.1080/11263500412331283762

Pérez-López D, Ribas F, Moriana A et al (2008) Influence of temperature on the growth and development of olive (Olea europaea L.) trees. J Hortic Sci Biotechnol 83:171–176. https://doi.org/10.1080/14620316.2008.11512366

Piñar Fuentes JCP, Cano-Ortiz A, Musarella CM et al (2019) Bioclimatology, structure, and conservation perspectives of Quercus pyrenaica, Acer opalus subsp. granatensis, and Corylus avellana

deciduous forests on Mediterranean bioclimate in the south-central part of the Iberian Peninsula. Sustainability 11(22):6500. https://doi.org/10.3390/su11226500

Rallo L, Martin GC (1991) The role of chilling in releasing olive floral buds from dormancy. J Am Soc Hortic Sci 116:1058–1062. https://doi.org/10.21273/jashs.116.6.1058

Ramos A, Rapoport HF, Cabello D, Rallo L (2018) Chilling accumulation, dormancy release temperature, and the role of leaves in olive reproductive budburst: evaluation using shoot explants. Sci Hortic-Amsterdam 231:241–252. https://doi.org/10.1016/J.SCIENTA.2017.11.003

Rhizopoulou S (2007) *Olea europaea* L. A botanical contribution to culture. Am J Agric Environ Sci 2:382–387

Riahi K, Rao S, Krey V et al (2011) RCP 8.5—a scenario of comparatively high greenhouse gas emissions. Clim Change 109:33–57. https://doi.org/10.1007/s10584-011-0149-y

Richardson E, Seeley S, Walker D (1974) A model for estimating the completion of rest for "Redhaven" and "Elberta" peach trees. Hortscience 9:331–332.https://doi.org/10.21273/HORTSCI.9.4.331

Rivas-Martínez S, Rivas-Saenz S, Penas A (2002) Worldwide bioclimatic classification system. Backhuys Pub, Universidad de León

Rivas-Martínez S, Pensas Á, del Río S, et al (2017) The vegetation of the Iberian Peninsula. In: Loidi J (ed) The vegetation of the Iberian Peninsula,Vol1, 1 edn. Springer

Rodríguez A, Pérez-López D, Sánchez E et al (2019) Chilling accumulation in fruit trees in Spain under climate change. Nat Hazards Earth Syst Sci 19:1087–1103. https://doi.org/10.5194/nhess-19-1087-2019

Rojo J, Orlandi F, Ben Dhiab A et al (2020) Estimation of chilling and heat accumulation periods based on the timing of olive pollination. Forests 11:835. https://doi.org/10.3390/f11080835

Santos JA, Costa R, Fraga H (2017) Climate change impacts on thermal growing conditions of main fruit species in Portugal. Clim Change 140:273–286. https://doi.org/10.1007/S10584-016-1835-6/FIGURES/5

Themeßl MJ, Gobiet A, Heinrich G (2011) Empirical-statistical downscaling and error correction of regional climate models and its impact on the climate change signal. Clim Change 112:449–468. https://doi.org/10.1007/s10584-011-0224-4

Torres M, Pierantozzi P, Searles P et al (2017) Olive cultivation in the Southern Hemisphere: flowering, water requirements and oil quality responses to new crop environments. Front Plant Sci 8:1830. https://doi.org/10.3389/fpls.2017.01830

Weinberger JH (1950) Chilling requirements of peach varieties. In: Proceedings. American Society for Horticultural Science. pp 122–128

Wise M, Calvin K, Thomson A et al (2009) Implications of limiting CO2 concentrations for land use and energy. Science 324:1183–1186. https://doi.org/10.1126/science.1168475

Wit C T de (1978) Simulation of assimilation, respiration and transpiration of crops. Pudoc, Wageningen

Zittis G, Hadjinicolaou P, Klangidou M et al (2019) A multi-model, multi-scenario, and multi-domain analysis of regional climate projections for the Mediterranean. Reg Environ Chang 19:2621–2635. https://doi.org/10.1007/s10113-019-01565-w

Zouari I, Mezghani A, Labidi F (2015) Flowering and heat requirements of four olive cultivars grown in the south of Tunisia. X Int Symp Model Fruit Res Orchard Manag 1160:231–236